

# DEVELOPMENT OF STCF HIGH-EFFICIENCY POSITRON CAPTURE TRAVELING WAVE ACCELERATING STRUCTURES\*

Z. Wang, J. Pang<sup>†</sup>, S. Ma, Q. Jin, A. Zhang, X. Xu  
University of Science and Technology of China, Hefei, China  
G. Pei, Institute of High Energy Physics, Beijing, China

## Abstract

The Super Tau-Charm Facility (STCF) is a next-generation electron-positron collider under development, with a designed center-of-mass energy of 2 GeV to 7 GeV. Positrons generated by a high-energy electron beam striking a target are captured and accelerated to 200 MeV using large-aperture traveling-wave accelerating structures to reduce beam loss. A constant-aperture cavity geometry, in which the group velocity is controlled by the nose-cone length, is proposed to simplify fabrication while maintaining a high accelerating gradient. A pulse compressor is incorporated into the RF system to further enhance the effective RF power. This paper presents the RF design and optimization of 2 m and 3 m large-aperture accelerating structures, both achieving gradients above 15 MV/m.

## INTRODUCTION

The Super Tau-Charm Facility (STCF) is a next-generation electron-positron collider designed for ultra-high luminosity operation, featuring high beam current, low emittance, and short beam lifetime. These characteristics impose stringent requirements on the injector and beam injection system.

STCF adopts a full-energy injection scheme, in which both electron and positron beams are accelerated by the linac to the storage-ring injection energy over the range of 1 GeV to 3.5 GeV. The facility operates in top-up mode, requiring continuous injection of high-charge, low-emittance beams at the specified repetition rate [1].

The positron beam is generated by a high-energy electron beam striking a target. Due to the large energy spread and poor beam quality of low-energy secondary positrons, conventional small-aperture structures provide low capture efficiency. To reduce beam loss and improve positron transmission efficiency, large-aperture traveling-wave accelerating structures are adopted.

Unlike conventional disk-loaded structures, the positron capture section employs constant-aperture accelerating structures with lengths of 2 m, 2 m, and 3 m, operating at gradients above 15 MV/m. This paper presents the RF design and optimization of these structures, including the RF system, operating mode, aperture, and cavity geometry.

\* This work is supported by the National Key R&D Program of China under Contract No. 2022YFA1602201. We also thank the Hefei Comprehensive National Science Center for their strong support on the STCF key technology research project.

<sup>†</sup> jpang@ustc.edu.cn

## RF SYSTEM

STCF operates primarily in single-pulse mode. Therefore, room-temperature traveling-wave accelerating structures with pulse compressors are adopted in the RF system [1]. To satisfy the high bunch-charge requirement, the linac operates at an S-band frequency of 2998.2 MHz.

A spherical pulse compressor with a dual-polarization-mode coupler is employed [2]. For a square input power envelope, the compressed output waveform exhibits exponential decay. Therefore, a shorter filling time results in a higher average accelerating gradient.

The pulse-compressor gain factor [3], defined as the ratio of the output voltage amplitude to the input voltage amplitude, is expressed as

$$M = \gamma e^{-T_a/T_c} \frac{1 - (1 - g)^{1+\nu}}{1 + \nu} - (\alpha - 1) \quad (1)$$

where  $T_a$  and  $T_c$  are the filling times of the accelerating structure and pulse-compressor cavity, respectively;  $g$  is the ratio of the residual output power to the input power of the accelerating structure and is related to the attenuation constant; and  $\alpha$  is determined by the coupling of the pulse-compressor storage cavity.

Microwave power is supplied by a single 40 MW klystron feeding two accelerating structures, with an estimated waveguide loss of 0.6 dB. The effective RF power is calculated using the pulse-compressor gain factor by Eq. 1.

## RF DESIGN OF LARGE-APERTURE LINAC STRUCTURE

### Mode Selection and Aperture Optimization

Compared with conventional disk-loaded waveguide structures, the proposed large-aperture accelerating structure adopts a constant-aperture geometry with chamfers on both sides of the iris. The group velocity and related RF parameters are controlled by varying the nose-cone length. A higher group velocity reduces the achievable accelerating field for a given input power, but shortens the filling time and increases the pulse-compressor gain. Therefore, the group velocity must be optimized to maximize the effective accelerating gradient.

Since both the operating mode and iris aperture affect the group velocity and RF performance, these parameters are optimized simultaneously. Four iris apertures,  $2a = 30$  mm, 40 mm, 50 mm and 60 mm, together with three operating modes,  $2\pi/3$ ,  $3\pi/4$ , and  $4\pi/5$ , are investigated.

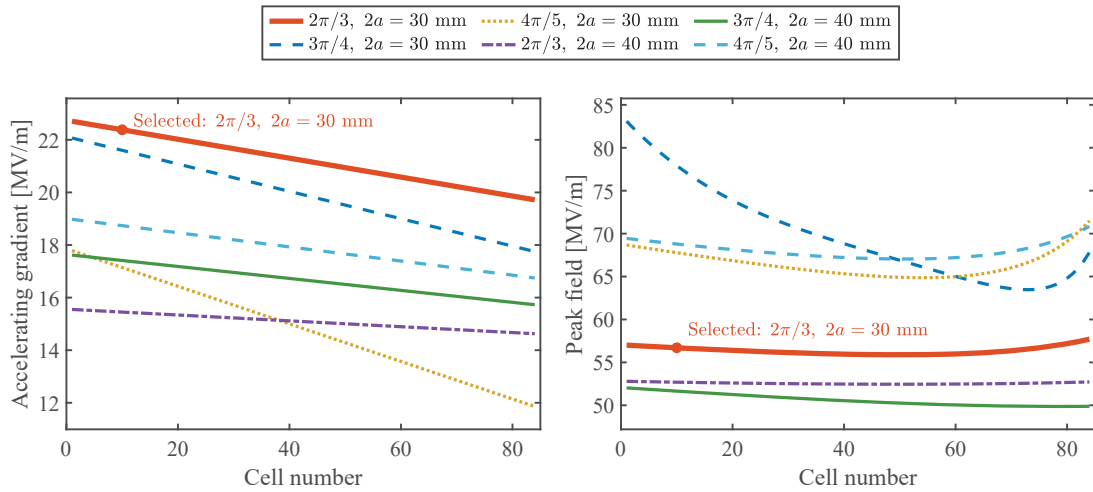


Figure 1: Accelerating gradient and peak field for different operating modes and iris apertures.

Table 1: Accelerating Gradient for Different Iris Apertures in the  $2\pi/3$  Mode

| Iris diameter [mm] | Accelerating gradient [MV/m] |
|--------------------|------------------------------|
| 30                 | 20.74                        |
| 40                 | 13.80                        |
| 50                 | 9.11                         |
| 60                 | 6.09                         |

A parameter scan is performed for all combinations. All RF parameters are calculated using SUPERFISH [4]. For the cases of  $2a = 50$  mm and  $60$  mm, the achievable accelerating gradients are significantly lower than the design target of  $15$  MV/m (Table 1). Neither changing the operating mode nor optimizing the cavity geometry can satisfy the gradient requirement.

The results for the  $2a = 30$  mm and  $40$  mm structures are shown in Fig. 1. Since the local field enhancement increases with nose-cone length, a linearly tapered gradient profile is adopted to equalize the breakdown risk along the structure. When the group velocity becomes excessively high, the increase in pulse-compressor gain cannot compensate for the reduction in shunt impedance. Among all configurations, the  $2a = 30$  mm structure operating in the  $2\pi/3$  mode achieves the highest average accelerating gradient while maintaining the low peak electric field. Therefore, this configuration is selected for the final design.

### Geometric Design of Regular Cells

In the design of the accelerating-structure cells, the main RF parameters of interest are the shunt impedance  $R_s$ , quality factor  $Q_0$ , and peak electric field  $E_{\text{peak}}$ . Higher  $R_s$  and  $Q_0$  improve the accelerating gradient and reduce RF power loss, while a lower  $E_{\text{peak}}$  decreases the breakdown probability and improves operational reliability. These parameters are mainly determined by the cavity geometry [5]. To optimize the RF performance while maintaining reasonable fabrica-

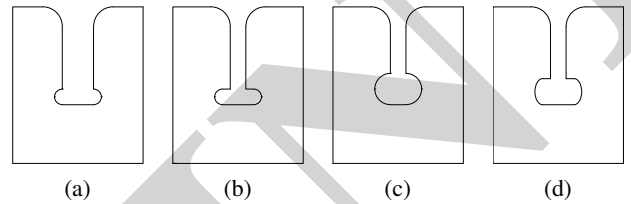


Figure 2: Comparison of different cavity geometries: (a) type1, (b) type2, (c) type3, and (d) type4.

tion complexity, four cavity geometries are investigated, as shown in Fig. 2.

Cavity type 1 is based on the FCC-ee positron accelerating structure design [6], in which the disk thickness varies with the nose-cone length over the range of  $7$  mm to  $12$  mm. The increased nose-cone volume reduces the shunt impedance and quality factor compared with conventional structures, resulting in higher RF loss. In addition, the large disk thickness increases the total structure weight, while the cell-to-cell geometric variation increases fabrication and brazing complexity.

Cavity types 2, 3, and 4 employ constant disk thickness. In cavity type 2, circular chamfers with constant radius are applied on both sides of the iris. In cavity type 3, the chamfer radius increases with nose-cone length instead of shifting the chamfer center position. In cavity type 4, elliptical chamfers with constant size are applied on both sides.

The RF performance of the four cavity types at the same average accelerating gradient are shown in Fig. 3. Cavity types 2, 3, and 4 exhibit higher shunt impedance than cavity type 1 as shown in Fig. 3(c), but also higher peak electric field as shown in Fig. 3(b). Compared with circular chamfers, the elliptical chamfer provides smoother electric-field transition near the iris edge, reducing local field enhancement. Among them, cavity type 4 has a peak field closest to that of cavity type 1, only  $8\%$  higher, while providing a smoother gradient profile and higher shunt impedance. Based on fabrication complexity and RF performance, cav-

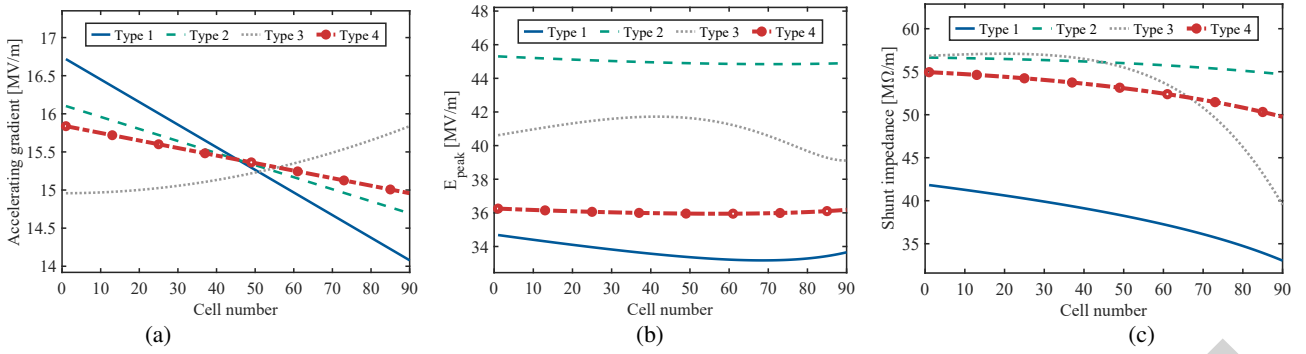


Figure 3: RF performance for different cavity types: (a) accelerating gradient, (b) peak field, and (c) shunt impedance.

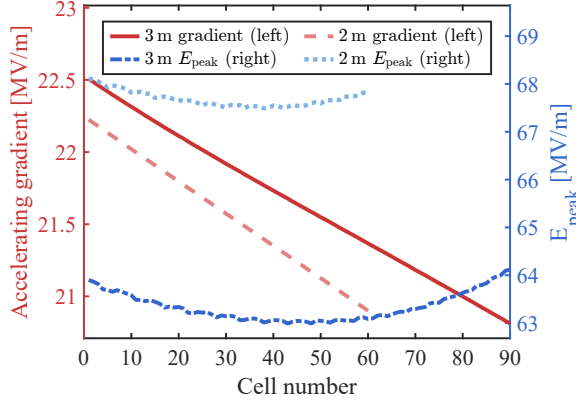


Figure 4: RF performance of optimized structures.

ity type 4 is chosen for the regular cells of the large-aperture accelerating structure.

### Final Structure Parameters

The design parameters of the large-aperture accelerating structure are summarized in Table 2. Pulse-compressed configurations are presented for the 2 m and 3 m structures, together with a 2 m structure operated without pulse compression, as shown in Fig. 4. The average accelerating gradients of the pulse-compressed structures exceed 21 MV/m, while the non-compressed 2 m structure achieves an average gradient of 16 MV/m.

The offset coupling scheme is adopted to minimize transverse field asymmetry for the large-aperture structure. The input coupler is designed using the three-frequency method. The output coupler is designed using the Kroll method, where undercoupling is adopted to suppress reflections [7].

## CONCLUSION

The RF design of the large-aperture accelerating structures for positron capture and acceleration in STCF has been completed. A pulse compressor is incorporated into the waveguide system to enhance the effective RF power delivered to the accelerating structures. The operating mode and iris aperture are optimized to achieve a balance between high accelerating gradient and low peak electric field, while the regular-cell geometry is optimized to improve the shunt impedance and RF performance.

Table 2: Design Parameters for Large-aperture Accelerating Structures

| Parameter  | 2 m structure | 3 m structure |
|--|---------------|---------------|
| Frequency [MHz]                                    | 2998.2        | 2998.2        |
| Operating temperature [°C]                         | 30            | 30            |
| Number of cells                                    | 60+2          | 90 + 2        |
| Length [mm]  | 2165          | 3165          |
| Iris diameter, $2a$ [mm]                           | 30            | 30            |
| Cell length [mm]                                   | 33.330        | 33.330        |
| Nose-cone length, $d$ [mm]                         | 9.34–11.97    | 8.42–12.33    |
| Shunt impedance [MΩ/m]                             | 53.27–48.45   | 54.37–47.60   |
| Quality factor                                     | 13 998–12 877 | 14 318–12 695 |
| Group velocity, $v_g/c$                            | 0.027–0.020   | 0.030–0.020   |
| Fill time [μs]                                     | 0.28          | 0.41          |
| Accelerating gradient [MV/m]                       | 16.10         | –             |
| Accelerating gradient with pulse compressor [MV/m] | 21.59         | 20.90         |

With the pulse compressor, the operating gradients of both the 2 m and 3 m structures exceed 21 MV/m. Without pulse compression, the 2 m structure achieves an operating gradient of approximately 16 MV/m. The proposed large-aperture accelerating structures provide an effective solution for high-efficiency positron capture and acceleration in STCF.

## REFERENCES

- [1] M. Achasov *et al.*, “STCF Conceptual Design Report (Volume 1): Physics and Detector,” *Front. Phys.*, vol. 19, no. 1, p. 1, 2023. doi:10.1007/s11467-023-1333-z
- [2] Z. Cao, Z. Huang, L. Sun, and Y. Wei, “RF Design of a C-Band Spherical Pulse Compressor for Linac of Super Tau-Charm Facility,” in *Proc. IPAC'24*, Nashville, TN, USA, May 2024, paper TUPR20. doi:10.18429/JACoW-IPAC2024-TUPR20
- [3] Z. D. Farkas, H. A. Hoag, G. A. Loew *et al.*, “SLED: A Method of Doubling SLAC’s Energy,” in *Proc. HEACC'74*, Stanford, CA, USA, 1974, pp. 576–583.
- [4] J. H. Billen and L. M. Young, “POISSON SUPERFISH,” LANL, NM, USA, Rep. LA-UR-96-1834, 1996.
- [5] Y. J. Pei, *Fundamentals of Electron Linear Accelerator Design*, Beijing, China: Science Press, 2013.
- [6] H. Pommerenke, A. Grudiev, A. Latina *et al.*, “RF Design of Traveling-Wave Accelerating Structures for the FCC-ee Pre-Injector Complex,” in *Proc. LINAC'22*, Liverpool, UK,

Aug.–Sep. 2022, paper THPOJO08.  
[doi:10.18429/JACoW-LINAC2022-THPOJO08](https://doi.org/10.18429/JACoW-LINAC2022-THPOJO08)

Light Facility,” *Rev. Sci. Instrum.*, vol. 95, no. 10, p. 103301,  
2024. [doi:10.1063/5.0208801](https://doi.org/10.1063/5.0208801)

- [7] S. Ma, F. Wu, Z. Wang *et al.*, “Design and Tuning of S-Band Traveling-Wave Accelerating Structures for Hefei Advanced

PREPRINT